Determining the validity of cumulant expansions for central spin models

Piper Fowler-Wright,[1] Kristín B. Arnardóttir,[1] Peter Kirton,[2] Brendon W. Lovett,[1] and Jonathan Keeling[1]

[1]*SUPA, School of Physics and Astronomy, University of St Andrews, St Andrews KY16 9SS, United Kingdom*

[2]*Department of Physics and SUPA, University of Strathclyde, Glasgow G4 0NG, United Kingdom*

(Received 8 March 2023; revised 12 June 2023; accepted 1 August 2023; published 1 September 2023)

For a model with many-to-one connectivity it is widely expected that mean-field theory captures the exact many-particle $N \to \infty$ limit, and that higher-order cumulant expansions of the Heisenberg equations converge to this same limit whilst providing improved approximations at finite N. Here we show that this is in fact not always the case. Instead, whether mean-field theory correctly describes the large-N limit depends on how the model parameters scale with N, and the convergence of cumulant expansions may be nonuniform across even and odd orders. Further, even when a higher-order cumulant expansion does recover the correct limit, the error is not monotonic with N and may exceed that of mean-field theory.

DOI: 10.1103/PhysRevResearch.5.033148

I. INTRODUCTION

Networks in which one site couples nonlocally to many satellite sites occur in a wide range of many-body open quantum systems. For example, models where a driven electronic spin interacts with a bath of nuclear spins are relevant to nuclear magnetic resonance spectroscopy [1–4], quantum sensing [5–7], and quantum information processing [8–14]. The network structure is also common in quantum optics where it defines the interaction of a bosonic mode with an ensemble of emitters [15], or equally a single emitter with many electromagnetic modes [16]. In many such cases, the large number of satellite sites precludes exact calculations, particularly when accounting for nonunitary dynamics due to incoherent processes. Consequently there is a need for approximate methods capable of handling large, driven-dissipative systems with many-to-one connectivity. We discuss below how mean-field theory and cumulant expansions may provide a suitable set of methods.

For models with finite connectivity, mean-field theory is typically only accurate in high dimensions [17]. In contrast, there are many reasons to believe it should recover the exact behavior of many-to-one models in the thermodynamic limit. First, given N identical satellites, monogamy of entanglement [18] restricts the entanglement between any two sites such that quantum correlations in the system vanish as $N \to \infty$. However, there is no similar restriction on *classical* correlations which may certainly persist in this limit. Second, in models with weak couplings to satellite sites, these may be treated as a harmonic bath for the central site with a linear response that becomes exact as $N \to \infty$ [19]. Third, for models with an interaction between a large number of emitters and a bosonic mode, the mean-field equations can be justified via saddle-point analysis [20]. There are further rigorous results regarding the exactness of mean-field theory as $N \to \infty$ within this class [21–23]. In spite of these results, we present here a simple example where mean-field theory does not always capture the $N \to \infty$ limit of a many-to-one model.

Even when mean-field theories correctly describe the exact $N \to \infty$ behavior, other methods may be required to capture effects at finite N. Different forms of cumulant expansion of the Heisenberg equations have been widely applied to many-body systems [16,24–39] as a systematic approximation scheme in which increasing orders of correlations are included; this is hoped to improve accuracy at the cost of growing complexity. The power of this approach is the small dimension of the resulting problem (independent of system size N), and the ability of even low orders of expansion to produce accurate results at intermediate N. Hence, they are a tool to both capture behavior at $N \gg 1$ and to study finite-size effects.

The difficulty of direct simulation at large N means that cumulant expansions are rarely benchmarked against exact methods much beyond $N \sim 30$. Confidence in results may then be based on the assumptions that evaluation at larger N and higher orders of expansion provide more accurate approximations. However, we show cases here where neither of these assumptions are correct.

In this work we thoroughly explore the convergence of cumulant expansions for a driven-dissipative central spin model. We demonstrate how the ability of mean-field theory to capture the $N \to \infty$ steady state of the full quantum model depends on the scaling of parameters. Further, we show how even when mean-field theory does capture the exact behavior at $N \to \infty$, convergence of higher-order cumulant expansions to the same result is not guaranteed. We discuss how this convergence behavior arises in light of correlations present in the system and show that similar behavior may be observed in models of light-matter interaction. Permutation symmetry

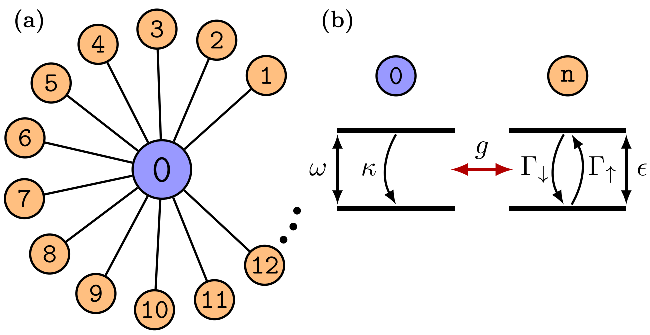

FIG. 1. (a) Network of the model: a central site (index 0) couples to N identical satellites ($n = 1, \dots, N$). (b) Each site is a two-level system (spin 1/2) subject to decay (κ or $\Gamma_\downarrow$) and, in the case of the satellites, pump $\Gamma_\uparrow$.

allows us to make comparisons to exact results for the central spin model at relatively large $N \sim 150$ whereby we show the error in cumulant expansion approximations does not generally decrease monotonically with N, nor with the order of expansion.

The structure of the paper is as follows. In Sec. II we give an overview of the central spin model and the permutation symmetric method that may be used to solve it at finite N. In Sec. III we explain the cumulant expansion method and its application to the model at mean field and second order. Section IV then compares the results for these approximations up to third order to exact data under two different choices for scaling of parameters as $N \to \infty$. Finally, in Sec. V we present the results for higher-order expansions in both the central spin and the Tavis-Cummings models before summarizing our findings and the scope for future work in Sec. VI.

II. MODEL

We consider a single spin 1/2 (Pauli matrices σ_0^α) interacting with N spin-1/2 satellites (Pauli matrices σ_n^α) according to

$$H = \frac{\omega}{2}\sigma_0^z + \sum_{n=1}^{N}\left[\frac{\epsilon}{2}\sigma_n^z + g(\sigma_0^+\sigma_n^- + \sigma_0^-\sigma_n^+)\right]. \quad (1)$$

Here ω and ϵ are on-site energies for the central and a satellite spin, and g the interaction strength. In addition we consider dissipation with rate κ from the central site as well as incoherent pump $\Gamma_\uparrow$ and loss $\Gamma_\downarrow$ for each satellite. These are included as Markovian terms in the master equation for the total density operator ρ,

$$\partial_t\rho = -i[H,\rho] + \kappa\mathcal{L}[\sigma_0^-] + \sum_{n=1}^{N}(\Gamma_\uparrow\mathcal{L}[\sigma_n^+] + \Gamma_\downarrow\mathcal{L}[\sigma_n^-]), \quad (2)$$

with $\mathcal{L}[x] = x\rho x^\dagger - \{x^\dagger x, \rho\}/2$. Schematics for the system and these processes are given in Figs. 1(a) and 1(b).

The anisotropic interactions in Eq. (1) arise, for example, between the nitrogen-vacancy center and the ^{13}C nuclear spins in diamond [40]. This system has been extensively studied for its potential role in emerging quantum technologies including spectroscopy [2–4], quantum sensing [5–7], and computing [12,13]. For our purpose the model serves a minimal formulation of the open many-to-one problem to investigate mean-field theory and cumulant expansions. In certain cases, such as the absence of dissipation, or when the satellite dissipation is collective, there exist analytical or efficient numerical methods capable of accessing large-N behavior of central spin models [41–46]. However, for the case we consider with individual dephasing these methods do not apply.

The model Eq. (2) has cumulant equations that are analytically tractable up to third order whilst also allowing exact calculations for relatively large system sizes. Below, to compare approximations, we analyze the central-site population, $p_0^\uparrow$, in the steady state. This relates to the polarization, $\langle\sigma_0^z\rangle$, via $p_0^\uparrow \equiv (1 + \langle\sigma_0^z\rangle)/2$ and increases from zero as the ratio $\Gamma_\uparrow/\Gamma_T$ ($\Gamma_T = \Gamma_\uparrow + \Gamma_\downarrow$) is increased.

The invariance of the model under the interchange of satellite spins allows one to work in a permutation-symmetric basis when performing exact calculations [47–52]. This provides a combinatoric reduction in the size of the Liouvillian L. In our case this allows finding the eigenvector of L with eigenvalue 0, i.e., the steady state, up to $N = 150$. No information is lost by working in this basis. In particular, all correlations can be computed exactly and compared to the prediction of the cumulant expansions.

III. MEAN-FIELD AND CUMULANT EXPANSIONS

We now explain the cumulant expansion method and its application to the central spin model at mean field and second order. Expressions for third-order cumulant equations are also provided in Appendix A.

From the master equation, Eq. (2), one can derive equations of motion for single-site expectations:

$$\partial_t\langle\sigma_0^z\rangle = -\kappa\left(\langle\sigma_0^z\rangle + 1\right) + 4gN\mathrm{Im}[\langle\sigma_0^+\sigma_n^-\rangle], \quad (3)$$

$$\partial_t\langle\sigma_n^z\rangle = -\Gamma_T\langle\sigma_n^z\rangle + \Gamma_\Delta - 4g\mathrm{Im}[\langle\sigma_0^+\sigma_n^-\rangle], \quad (4)$$

$$\partial_t\langle\sigma_0^+\rangle = \left(i\omega - \frac{\kappa}{2}\right)\langle\sigma_0^+\rangle - igN\langle\sigma_0^z\sigma_n^+\rangle, \quad (5)$$

$$\partial_t\langle\sigma_n^+\rangle = \left(i\epsilon - \frac{\Gamma_T}{2}\right)\langle\sigma_n^+\rangle - ig\langle\sigma_0^+\sigma_n^z\rangle, \quad (6)$$

where $\Gamma_\Delta = \Gamma_\uparrow - \Gamma_\downarrow$ and $\Gamma_T = \Gamma_\uparrow + \Gamma_\downarrow$. This set of equations is not closed since, for example, $\partial_t\langle\sigma_0^z\rangle$ depends on $\langle\sigma_0^+\sigma_n^-\rangle$. The equation for $\langle\sigma_0^+\sigma_n^-\rangle$ will in turn depend on expectations of operators from three different sites, and so on, resulting in an exponential number of equations involving operators on all sites.

To obtain a manageable number of equations, in the Mth-order cumulant expansion moments of order $M+1$ are rewritten as nonlinear combinations of lower-order moments by setting the corresponding *cumulant* [24,53] to zero. Such an approximation corresponds to making an ansatz for the many-body state ρ that involves correlations between at most M sites. We stress here the distinction is between sites (or Hilbert spaces) of the many-body system, not operators in themselves (as, e.g., used in Ref. [28]). This is natural for two-level systems, where one easily identifies $\langle\sigma_0^+\sigma_0^-\sigma_n^z\rangle = (\langle\sigma_0^z\sigma_n^z\rangle + \langle\sigma_n^z\rangle)/2$, but for bosonic operators,

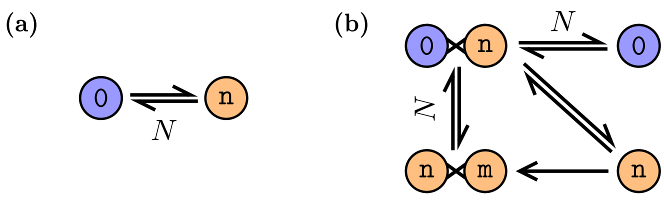

FIG. 2. (a) Mean-field reduction to a two-body problem where expectations of a satellite evolve according to expectations of the central site ($\rightharpoonup$) which in turn evolve according to N copies of the satellite expectations ($\leftharpoondown$). (b) In the second-order cumulant expansion central-satellite and satellite-satellite expectations couple into the system [Eqs. (10) and (11)].

e.g., a, it is common to see factorizations such as $\langle a^\dagger a \sigma^z\rangle \approx \langle a^\dagger\rangle\langle a\rangle\langle\sigma^z\rangle + \cdots$ whose validity depends on additional assumptions of Gaussianity [54].

A. Mean-field equations

At first order, that is mean-field theory, second-order moments factorize into products ($\langle\sigma_0^\alpha\sigma_n^\beta\rangle \approx \langle\sigma_0^\alpha\rangle\langle\sigma_n^\beta\rangle$) and an effective two-body problem results [Fig. 2(a)]. Solving for the steady state one finds $\langle\sigma_0^z\rangle = -1$ for $\Gamma_\uparrow/\Gamma_T$ below a critical pump ratio $R_c \equiv (1 + \Gamma_T\kappa/4g^2N)/2$, while for $\Gamma_\uparrow/\Gamma_T > R_c$,

$$\langle\sigma_0^z\rangle = -\frac{1}{2}\left(1 - \frac{\Gamma_\Delta N}{\kappa}\right) - \frac{1}{2}\sqrt{\left(1 - \frac{\Gamma_\Delta N}{\kappa}\right)^2 + \frac{\Gamma_T^2}{g^2}}, \tag{7}$$

$$\langle\sigma_n^z\rangle = -\frac{\kappa\Gamma_T}{4g^2N\langle\sigma_0^z\rangle}, \quad \langle\sigma_n^+\rangle = \frac{i\kappa}{2gN\langle\sigma_0^z\rangle}\langle\sigma_0^+\rangle, \tag{8}$$

where the magnitude of $\langle\sigma_0^+\rangle$ is fixed by

$$|\langle\sigma_0^+\rangle|^2 = -\langle\sigma_0^z\rangle\left(1 + \langle\sigma_0^z\rangle\right)/2. \tag{9}$$

For simplicity we took $\omega = \epsilon$ above but have checked our conclusions do not change off resonance.

Although the model has U(1) symmetry, i.e., Eq. (2) is invariant under $\sigma^\pm \to \sigma^\pm e^{\pm i\theta}$, it is necessary to retain the symmetry-breaking terms $\langle\sigma_0^+\rangle$ and $\langle\sigma_n^+\rangle$ when performing the mean-field approximation in order to obtain a nontrivial solution: the state $\langle\sigma_0^z\rangle = -1$ is always a solution to the mean-field equations that only becomes unstable when $\Gamma_\uparrow/\Gamma_T > R_c$.

B. Second-order cumulant equations

Breaking symmetry is not necessary at second order where $\langle\sigma_0^+\sigma_n^-\rangle$ can be nonzero whilst respecting the symmetry. The required equations for second moments are [Fig. 2(b)]

$$\partial_t\langle\sigma_0^+\sigma_n^-\rangle = \left(i(\omega-\epsilon) - \frac{\kappa+\Gamma_T}{2}\right)\langle\sigma_0^+\sigma_n^-\rangle + \frac{ig}{2}\langle\sigma_n^z\rangle - \frac{ig}{2}\langle\sigma_0^z\rangle - ig(N-1)\langle\sigma_0^z\rangle\langle\sigma_n^+\sigma_m^-\rangle, \tag{10}$$

$$\partial_t\langle\sigma_n^+\sigma_m^-\rangle = -\Gamma_T\langle\sigma_n^+\sigma_m^-\rangle + 2g\mathrm{Im}[\langle\sigma_0^+\sigma_n^-\rangle]\langle\sigma_n^z\rangle, \tag{11}$$

with $n \neq m$. Here we set third cumulants to zero and use the U(1) symmetry to write $\langle\sigma_0^z\sigma_n^+\sigma_m^-\rangle \approx \langle\sigma_0^z\rangle\langle\sigma_n^+\sigma_m^-\rangle$, $\langle\sigma_0^+\sigma_n^-\sigma_m^z\rangle \approx \langle\sigma_0^+\sigma_n^-\rangle\langle\sigma_n^z\rangle$. Equations (3), (4), (10), and (11) can also be solved exactly, albeit not explicitly, to find $p_0^\uparrow = [1 + \langle\sigma_0^z\rangle]/2$.

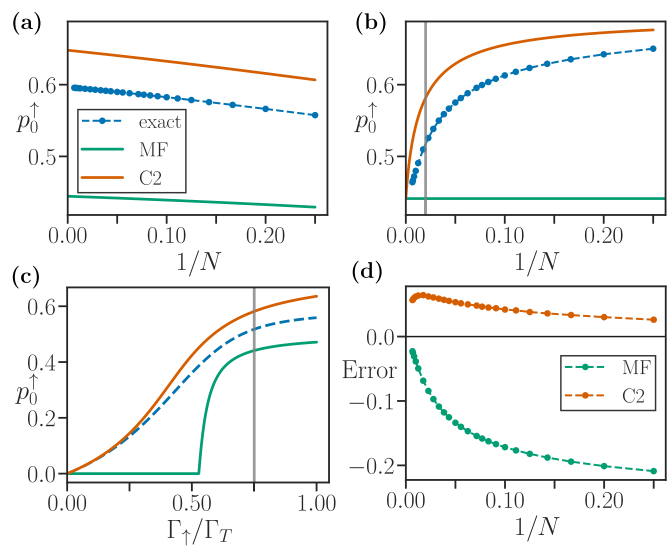

FIG. 3. (a) Central-site population, $p_0^\uparrow = [1 + \langle\sigma_0^z\rangle]/2$, in mean-field (MF) and second-order cumulant (C2) approximations when $g\sqrt{N} = 3$ is fixed and $\kappa = 1$ in units of ω. Exact data (blue dots) is included up to $N = 150$. The horizontal scale $1/N$ is such that $N \to \infty$ to the left. (b) MF, C2, and exact results when $\kappa/N = 1/16$ is fixed and $g = 3/4$. The gray vertical line at $N = 50$ indicates points equivalent to those along the corresponding line in (c). (c) $p_0^\uparrow$ vs $\Gamma_\uparrow/\Gamma_T$ ($\Gamma_T = \Gamma_\uparrow + \Gamma_\downarrow$) at fixed $\kappa/N = 1/16$, $g = 3/4$, and $N = 50$ (the low cost of the exact calculation allowed a continuous line to be plotted). The mean-field transition at $\Gamma_\uparrow/\Gamma_T = R_c \approx 0.53$ is analogous to that in a driven-dissipative Tavis-Cummings model [15] and other models of lasing [37,55]. (d) Error in MF and C2 results from (b). Other parameters used in these panels were $\epsilon = \omega = 1$, $\Gamma_T = 2$, and [except (c)] $\Gamma_\uparrow = 3/2$.

IV. RESULTS AT MEAN-FIELD AND SECOND-ORDER CUMULANTS

In the following we compare the mean-field result, Eq. (7), and the solution to the second-order equations, Eqs. (3), (4), (10), and (11), to the exact steady state. We do this this under two possible choices for scaling parameters in the model as $N \to \infty$.

A. Fixed $g\sqrt{N}$

Figure 3(a) shows $p_0^\uparrow$ vs $1/N$ when fixing $g\sqrt{N}$. This scaling is often relevant in the context of light-matter coupling, where coupling strength g is inversely proportional to the square root of mode volume: as the system becomes larger, both N and mode volume grow, but $g\sqrt{N}$ remains fixed. Here we see there is no agreement between the exact and approximate results, each taking different $N \to \infty$ limits. This is in marked contrast to the Tavis-Cummings or Dicke models [51], where both mean-field and second-order cumulant approximations converge to the exact steady-state as $N \to \infty$ for this scaling. Below we explain how the convergence of second-order cumulants to mean-field theory is precluded by $g \propto 1/\sqrt{N}$ for the central spin model.

B. Fixed κ/N

If instead the ratio κ/N is kept fixed [Fig. 3(b)], mean-field and second-order cumulants have a common limit that captures the exact behavior. Note Fig. 3(b) is plotted for parameters where nonzero $p_0^\uparrow$ is expected [see Fig. 3(c) for a phase diagram]. This scaling may be understood to realize the limit of strong continuous measurement of the central site [56]. It has the feature, seen in Eqs. (7)–(9), that expectations of satellite and central-site quantities are of the same order, $O(1)$, as $N \to \infty$. In Appendix B we show this holds for higher-order correlations as well. One then observes the asymptotic form of Eq. (10) ($\kappa \sim N$),

$$\partial_t \langle \sigma_0^+ \sigma_n^- \rangle = N\left(-\frac{\kappa}{2N}\langle \sigma_0^+ \sigma_n^- \rangle - ig\langle \sigma_0^z \rangle \langle \sigma_n^+ \sigma_m^- \rangle\right) + O(1), \tag{12}$$

matches that predicted by mean-field theory,

$$\partial_t(\langle \sigma_0^+ \rangle \langle \sigma_n^- \rangle) = N\left(-\frac{\kappa}{2N}\langle \sigma_0^+ \rangle \langle \sigma_n^- \rangle - ig\langle \sigma_0^z \rangle \langle \sigma_n^+ \rangle \langle \sigma_m^- \rangle\right) + O(1). \tag{13}$$

The same is true for Eq. (11) and its mean-field analog, hence the second-order and mean-field equations have identical structures as $N \to \infty$ at fixed κ/N.

In contrast, at fixed $g\sqrt{N}$ the correlations $\langle \sigma_n^+ \sigma_m^- \rangle$ do not remain finite as $N \to \infty$ but decay faster than $1/\sqrt{N}$ (Appendix B). Consequently the terms $\sim g\langle \sigma_0^z \rangle$, $g\langle \sigma_n^z \rangle$ in Eq. (10), which are not present in mean-field theory, cannot be discounted as $N \to \infty$. This difference leads to distinct limits in Fig. 3(a). Note equations for higher-order moments involving the central site will contain additional terms inconsistent with mean-field theory. Thus, while higher-order expansions *may* provide an improved approximation of the exact results, they will generally have distinct limits. This result also illustrates how knowledge that certain correlations vanish at large N is not sufficient to determine if they become irrelevant as $N \to \infty$. Instead, the scaling with N of parameters multiplying these correlations must also be taken into account.

Figure 3(d) shows further how with κ/N fixed the error at second order is not monotonic with N and even exceeds that of mean-field theory for $N \gtrsim 80$. The nonmonotonicty is inevitable given this approach captures the exact $N \to \infty$ limit and must also be exact at $N = 2$, when all correlations are fully captured. As such, the second-order expansion provides an approximation that is only asymptotically matched to the exact result at the two limits, and care must be taken in between.

V. HIGHER-ORDER CUMULANT EXPANSIONS

A. Central spin model

Having established a well-defined limit up to second order at fixed κ/N, we now investigate higher-order cumulant expansions for this scaling. We use the QuantumCumulants.jl Julia framework [35] to obtain fourth- and fifth-order results in addition to the solution to the third-order equations presented in Appendix A. Surprisingly, we see in Fig. 4(a) that whilst the fourth-order expansion provides an improved approximation on the entire range of N, the third-order expansion does not. Instead it converges to a limit far separated from the true result, hence there is some N beyond which the second-order (and mean-field) result provides a better approximation. Similarly the fifth-order result, despite being exact up to $N = 5$ and the best approximation at very small N, fails to capture the exact $N \to \infty$ limit.

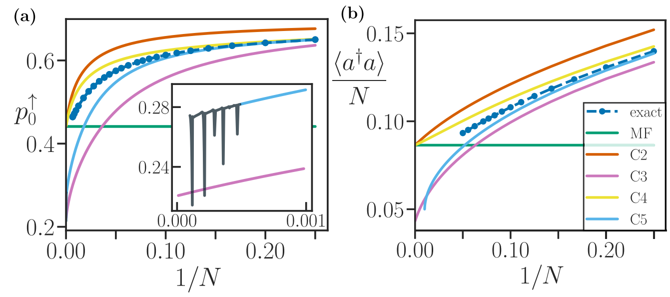

FIG. 4. (a) Central-site population $p_0^\uparrow$ in mean-field (MF) and cumulant approximations up to fifth order (C2-5) at fixed $\kappa/N = 1/16$ [parameters and exact data as in Fig. 3(b)]. Results at fourth and fifth order were derived using QuantumCumulants.jl [35]. Inset: the fifth-order solution has numerical noise beyond $N \gtrsim 2,500$, but is approaching a value distinct from the third-order limit. (b) Mean-field and cumulant results for the scaled photon number $\langle a^\dagger a \rangle/N$ in the driven-dissipative Tavis-Cummings model using QuantumCumulants.jl. Exact results following a Fock-space truncation are included up to $N = 20$ ($N_{\text{phot.}} = 20$ levels were sufficient to achieve convergence). Here the parameters were $g\sqrt{N} = 9/10$, $\epsilon = \omega = \kappa = 1$, $\Gamma_T = 1/2$, and $\Gamma_\uparrow = 3\Gamma_T/4$. The fifth-order solution became unstable for $N \gtrsim 100$.

To understand the dependence of convergence on order parity, the previous argument for the asymptotic reduction of the second-order equations to mean field as $N \to \infty$ can be extended to all even orders. First, note that before any factorization is made the equations for moments involving satellite sites only match mean-field theory in structure since H [Eq. (1)] is linear in these sites. When the central site is involved, this is no longer the case. However, the terms that survive as $N \to \infty$ at fixed κ/N are those that arise from the commutator of a central operator with $\sigma_0^+\sigma_n^-$ or $\sigma_0^-\sigma_n^+$ followed by a sum $\sim N$ over the satellites. These terms have the same structure for both the cumulant equations and mean-field theory. Second, there is a key point about the coefficients associated with the cumulant expansion of a given term. As discussed further in Appendix C, by definition, the sum of coefficients of the cumulant expansion of any given term should sum to 1. However, when some terms are eliminated because they do not respect the symmetries of the model, this statement may or may not remain true. When moments are factorized at even orders of expansion, the number of nonvanishing terms under U(1) symmetry does sum to 1 [57]. As this matches the mean-field prediction for the number of terms, the asymptotic structure of even-order equations are compatible with mean-field theory.

On the other hand, closing the equations at odd orders requires factorizing moments $\langle \sigma_0^+ \sigma_n^- \sigma_m^+ \sigma_k^- \dots \rangle$ involving raising and lowering operators only. These produce a set of terms with coefficients that do *not* sum to 1. For example, when constructing the third-order equations setting the cumulant $\langle\langle\sigma_0^+\sigma_n^-\sigma_m^+\sigma_k^-\rangle\rangle$ to zero gives

$$\langle\sigma_0^+\sigma_n^-\sigma_m^+\sigma_k^-\rangle \approx 2\langle\sigma_0^+\sigma_n^-\rangle\langle\sigma_m^+\sigma_k^-\rangle, \tag{14}$$

having excluded terms that vanish on account of the U(1) symmetry. It is the factor of 2 occurring here that is incongruent with mean-field theory. The number of terms produced by these type of factorizations varies with successive odd orders $(2, -3, 34, -455\ldots)$, so each can be expected to converge on its own limiting value at $N \to \infty$, as observed in Fig. 4(a) for third and fifth orders.

A consequence of these observations is that symmetry-broken versions of the odd-order equations, for which no terms of the approximation for $\langle\sigma_0^+\sigma_n^-\sigma_m^+\sigma_k^-\ldots\rangle$ vanish, can produce the correct limit. In Appendix C we show this is indeed the case for our model. However, we note that at finite N the exact solution never shows symmetry breaking, and that the symmetry-broken approximation is not necessarily a reliable improvement.

B. Tavis-Cummings model

Finally we observe similar convergence behavior between even and odd orders in models of light-matter interaction. Figure 4(b) includes results for the driven-dissipative Tavis-Cummings model up to fifth order of the cumulant expansion [58]. The Tavis-Cummings Hamiltonian [59] is frequently used in cavity QED to describe an ensemble of noninteracting emitters coupled to a common cavity mode and may be obtained from Eq. (1) by replacing the central spin with a bosonic operator a [15]. Note for this model $g\sqrt{N}$ fixed provides matching exact and mean-field $N \to \infty$ limits for the steady state [51].

VI. DISCUSSION

In this paper we examined the convergence of mean-field and cumulant expansions at $N \to \infty$ as well as their accuracy at intermediate N. We considered the class of all-to-one models for which mean-field theory may be expected to be robust. Yet for our central spin model we demonstrated that whether mean-field theory captures the exact steady state as $N \to \infty$ depends on the scaling of parameters in the model. Further, even when mean-field theory does capture exact $N \to \infty$ behavior, higher-order cumulant expansions may not converge to the same result. Comparison to exact results up to $N = 150$ allowed us to verify the large-N behavior and show the error of cumulant expansions is not monotonic with N.

The model considered here has been directly applied to study defect centers in diamond [2,3,60] and quantum dot systems [60,61], but our reasoning may be applied quite generally to central spin models including, for example, other anisotropic or isotropic couplings [62–65] or coherent drive [55,66,67]. We have also seen that our results are relevant to models of collective light-matter coupling where cumulant expansions are an increasingly popular choice for analyzing both small and large systems [16,30–37].

While we focused on steady-state properties, future work may use the cumulant expansions to examine the dynamics of open central spin models [65,68–72] for which the scope of mean-field theory to capture exact $N \to \infty$ behavior has recently been studied [23,73]. Similarly, one may look to apply our reasoning to models with all-to-all connectivity considering studies [29,33,36,39,74] of the limitations of mean-field approximations in this class. Our results highlight the need to assess the validity of cumulant expansions in such applications, and prompt further exploration of how reliable higher-order expansions can be found.

Note added. Recently, another work studying this same problem has appeared [73].

The research data supporting this publication can be accessed at Ref. [75].

ACKNOWLEDGMENTS

The authors thank Federico Carollo for valuable discussions. P.F.-W. acknowledges support from EPSRC (Grant No. EP/T518062/1). K.B.A, B.W.L., and J.K. acknowledge support from EPSRC (Grant No. EP/T014032/1).

APPENDIX A: THIRD-ORDER CUMULANT EQUATIONS

In this Appendix we provide the third-order cumulant equations for the central spin model with U(1) symmetry. In the following, n, m, and k label distinct satellite sites.

$$\partial_t\langle\sigma_0^z\rangle = -\kappa\left(\langle\sigma_0^z\rangle + 1\right) + 4gN\text{Im}[\langle\sigma_0^+\sigma_n^-\rangle], \tag{A1}$$

$$\partial_t\langle\sigma_n^z\rangle = -\Gamma_T\langle\sigma_n^z\rangle + \Gamma_\Delta - 4g\text{Im}[\langle\sigma_0^+\sigma_n^-\rangle], \tag{A2}$$

$$\partial_t\langle\sigma_0^+\sigma_n^-\rangle = \left(i(\omega-\epsilon) - \frac{\kappa+\Gamma_T}{2}\right)\langle\sigma_0^+\sigma_n^-\rangle + \frac{ig}{2}\langle\sigma_n^z\rangle - \frac{ig}{2}\langle\sigma_0^z\rangle - ig(N-1)\langle\sigma_0^z\sigma_n^+\sigma_m^-\rangle, \tag{A3}$$

$$\partial_t\langle\sigma_n^+\sigma_m^-\rangle = -\Gamma_T\langle\sigma_n^+\sigma_m^-\rangle + 2g\text{Im}\left[\langle\sigma_0^+\sigma_n^-\sigma_m^z\rangle\right], \tag{A4}$$

$$\partial_t\langle\sigma_0^z\sigma_n^+\sigma_m^-\rangle = -(\kappa+\Gamma_T)\langle\sigma_0^z\sigma_n^+\sigma_m^-\rangle - \kappa\langle\sigma_n^+\sigma_m^-\rangle + 2g\text{Im}[\langle\sigma_0^+\sigma_n^-\rangle] + 8g(N-2)\text{Im}[\langle\sigma_0^+\sigma_n^-\rangle]\langle\sigma_n^+\sigma_m^-\rangle, \tag{A5}$$

$$\begin{aligned}\partial_t\langle\sigma_0^+\sigma_n^-\sigma_m^z\rangle = &\left(i(\omega-\epsilon) - \frac{\kappa+3\Gamma_T}{2}\right)\langle\sigma_0^+\sigma_n^-\sigma_m^z\rangle + \Gamma_\Delta\langle\sigma_0^+\sigma_n^-\rangle - ig\langle\sigma_n^+\sigma_m^-\rangle + \frac{ig}{2}\langle\sigma_n^z\sigma_m^z\rangle - \frac{ig}{2}\langle\sigma_0^z\sigma_n^z\rangle\\ &- ig(N-2)\left(\langle\sigma_0^z\sigma_n^+\sigma_m^-\rangle\langle\sigma_n^z\rangle + \langle\sigma_0^z\rangle\langle\sigma_n^z\sigma_m^+\sigma_k^-\rangle + \langle\sigma_0^z\sigma_n^z\rangle\langle\sigma_n^+\sigma_m^-\rangle - 2\langle\sigma_0^z\rangle\langle\sigma_n^z\rangle\langle\sigma_n^+\sigma_m^-\rangle\right),\end{aligned} \tag{A6}$$

$$\begin{aligned}\partial_t\langle\sigma_n^z\sigma_m^+\sigma_k^-\rangle = &-2\Gamma_T\langle\sigma_n^z\sigma_m^+\sigma_k^-\rangle + \Gamma_\Delta\langle\sigma_n^+\sigma_m^-\rangle - 8g\text{Im}[\langle\sigma_0^+\sigma_n^-\rangle]\langle\sigma_n^+\sigma_m^-\rangle\\ &+ 2g\left(\text{Im}[\langle\sigma_0^+\sigma_n^-\rangle]\langle\sigma_n^z\sigma_m^z\rangle - 2\text{Im}[\langle\sigma_0^+\sigma_n^-\rangle]\langle\sigma_n^z\rangle^2 + 2\text{Im}\left[\langle\sigma_0^+\sigma_n^-\sigma_m^z\rangle\right]\langle\sigma_n^z\rangle\right),\end{aligned} \tag{A7}$$

$$\partial_t\langle\sigma_n^z\sigma_m^z\rangle = -2\Gamma_T\langle\sigma_n^z\sigma_m^z\rangle + 2\Gamma_\Delta\langle\sigma_n^z\rangle - 8g\mathrm{Im}\left[\langle\sigma_0^+\sigma_n^-\sigma_m^z\rangle\right], \tag{A8}$$

$$\partial_t\langle\sigma_0^z\sigma_n^z\rangle = -(\kappa+\Gamma_T)\langle\sigma_0^z\sigma_n^z\rangle - \kappa\langle\sigma_n^z\rangle + \Gamma_\Delta\langle\sigma_0^z\rangle + 4g(N-1)\mathrm{Im}\left[\langle\sigma_0^+\sigma_n^-\sigma_m^z\rangle\right]. \tag{A9}$$

In writing Eqs. (A5)–(A7) fourth-order moments were approximated by setting the fourth-order cumulants to zero:

$$\langle\langle\sigma_0^+\sigma_n^-\sigma_m^+\sigma_k^-\rangle\rangle = 0, \quad \langle\langle\sigma_0^z\sigma_n^z\sigma_m^+\sigma_k^-\rangle\rangle = 0, \quad \langle\langle\sigma_0^+\sigma_n^-\sigma_m^z\sigma_k^z\rangle\rangle = 0, \tag{A10}$$

where

$$\begin{aligned}\langle\langle\sigma_a^\alpha\sigma_b^\beta\sigma_c^\gamma\sigma_d^\delta\rangle\rangle := {}& \langle\sigma_a^\alpha\sigma_b^\beta\sigma_c^\gamma\sigma_d^\delta\rangle - \langle\sigma_a^\alpha\sigma_b^\beta\rangle\langle\sigma_c^\gamma\sigma_d^\delta\rangle - \langle\sigma_a^\alpha\sigma_c^\gamma\rangle\langle\sigma_b^\beta\sigma_d^\delta\rangle - \langle\sigma_a^\alpha\sigma_d^\delta\rangle\langle\sigma_b^\beta\sigma_c^\gamma\rangle \\ & - \langle\sigma_a^\alpha\rangle\langle\sigma_b^\beta\sigma_c^\gamma\sigma_d^\delta\rangle - \langle\sigma_b^\beta\rangle\langle\sigma_a^\alpha\sigma_c^\gamma\sigma_d^\delta\rangle - \langle\sigma_a^\alpha\sigma_b^\beta\sigma_d^\delta\rangle\langle\sigma_c^\gamma\rangle - \langle\sigma_a^\alpha\sigma_b^\beta\sigma_c^\gamma\rangle\langle\sigma_d^\delta\rangle \\ & + 2\langle\sigma_a^\alpha\rangle\langle\sigma_b^\beta\rangle\langle\sigma_c^\gamma\sigma_d^\delta\rangle + 2\langle\sigma_a^\alpha\rangle\langle\sigma_b^\beta\sigma_c^\gamma\rangle\langle\sigma_d^\delta\rangle + 2\langle\sigma_a^\alpha\rangle\langle\sigma_b^\beta\sigma_d^\delta\rangle\langle\sigma_c^\gamma\rangle \\ & + 2\langle\sigma_a^\alpha\sigma_b^\beta\rangle\langle\sigma_c^\gamma\rangle\langle\sigma_d^\delta\rangle + 2\langle\sigma_a^\alpha\sigma_c^\gamma\rangle\langle\sigma_b^\beta\rangle\langle\sigma_d^\delta\rangle + 2\langle\sigma_a^\alpha\sigma_d^\delta\rangle\langle\sigma_b^\beta\rangle\langle\sigma_c^\gamma\rangle - 6\langle\sigma_a^\alpha\rangle\langle\sigma_b^\beta\rangle\langle\sigma_c^\gamma\rangle\langle\sigma_d^\delta\rangle.\end{aligned} \tag{A11}$$

Note that many of these terms vanish for the model with U(1) symmetry.

APPENDIX B: BEHAVIOR OF CORRELATIONS AS $N \to \infty$

In this Appendix we show the behavior of pairwise correlations as $N \to \infty$ for the central spin model. These results support the arguments for convergence made in Sec. IV B.

Figures 5(a) and 5(b) show satellite-satellite $\langle\sigma_n^+\sigma_m^-\rangle$ and central-satellite $\langle\sigma_0^+\sigma_n^-\rangle$ correlations against $1/\sqrt{N}$ for the model at fixed $g\sqrt{N}$. We show exact results up to $N = 150$ as well as the prediction of second-order cumulants and mean-field theory. Notice in particular that $\langle\sigma_n^+\sigma_m^-\rangle$ decays faster than $1/\sqrt{N}$ as $N \to \infty$ [vanishing gradient at $1/\sqrt{N} \to 0$ in Fig. 5(a)]. As such, at large N, the terms $\sim g\langle\sigma_0^z\rangle$, $\sim g\langle\sigma_n^z\rangle$ present in the second-order equation, Eq. (10)

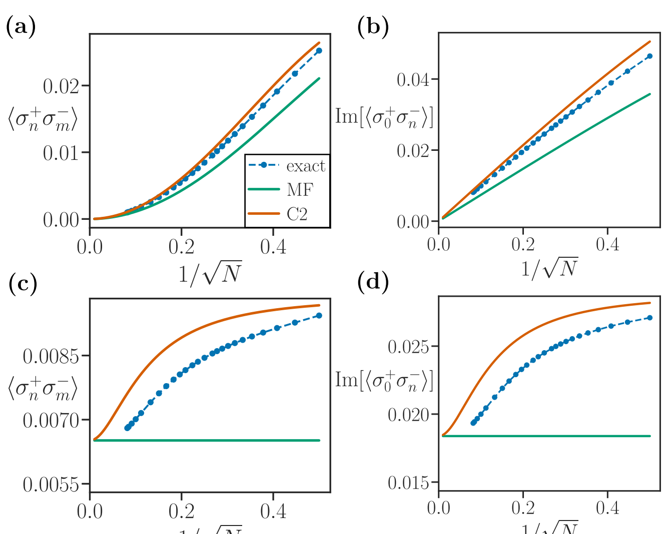

FIG. 5. (a) Satellite-satellite and (b) central-satellite correlations in the steady state of the model with scaling $g\sqrt{N}$ fixed and parameters as in Fig. 3(a) ($g\sqrt{N} = 3$, $\kappa = 1$). Exact data (blue dots) up to $N = 150$ and second-order (C2) results for the correlations are included, as well as the mean-field (MF) approximations $\langle\sigma_n^+\sigma_m^-\rangle \approx |\langle\sigma_n^+\rangle|^2$ and $\langle\sigma_0^+\sigma_n^-\rangle \approx \langle\sigma_0^+\rangle\langle\sigma_n^-\rangle$. Note the use of $1/\sqrt{N}$ on the horizontal axis: for this scaling $\langle\sigma_n^+\sigma_m^-\rangle = o(1/\sqrt{N})$ and $\mathrm{Im}\,[\langle\sigma_0^+\sigma_n^-\rangle] = O(1/\sqrt{N})$ as $N \to \infty$ (the real part of $\langle\sigma_0^+\sigma_n^-\rangle$ vanishes at resonance). (c), (d) Same correlations when instead κ/N is fixed with parameters as in Fig. 3(b) ($\kappa/N = 1/16$, $g = 3/4$). In this case both pairs of correlations remain finite for all N.

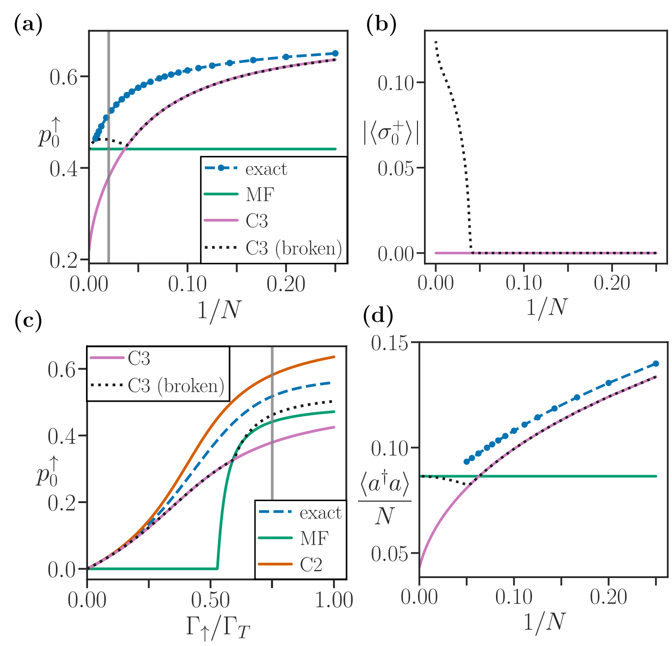

FIG. 6. (a) Exact, mean-field (MF), and third-order (C3) results for the steady-state central-site population $p_0^\uparrow = [1 + \langle\sigma_0^z\rangle]/2$ of the central spin model at fixed κ/N [parameters as in Fig. 3(b): $\kappa/N = 1/16$, $g = 3/4$]. Third-order results retaining symmetry-breaking terms in the equations are indicated with a dotted black line. (b) At $N = 26$ symmetry breaking $\langle\sigma_0^+\rangle \neq 0$ occurs in the steady state of these equations corresponding to the turning point of the dotted line in (a). (c) Central population versus $\Gamma_\uparrow/\Gamma_T$ ($\Gamma_T = \Gamma_\uparrow + \Gamma_\downarrow$) at $N = 50$ as in Fig. 3(c) ($\kappa/N = 1/16$, $g = 3/4$), now including third-order results with and without symmetry-breaking terms. The gray vertical line indicates data from (a). (d) Exact, mean-field (MF), and third-order (C3) results for the scaled photon number in the Tavis-Cummings model with parameters as in Fig. 4(b) ($g\sqrt{N} = 9/10$, $\Gamma_\uparrow = 3\Gamma_T/4$).

(but not mean-field theory), are dominant compared to the final term $\sim g\langle\sigma_0^z\rangle\langle\sigma_n^+\sigma_m^-\rangle$ occurring there.

When instead considering the correlations at fixed κ/N, shown in Figs. 5(c) and 5(d), we see that both tend to finite limits, allowing for the reduction of the second-order cumulant equations to mean-field theory when $N\to\infty$ as argued in the main text.

Thus we have both a case where correlations vanish as $N\to\infty$ but mean-field and second-order cumulants do not have a well-defined limit [Fig. 3(a)], and a case where they remain finite yet the two approaches have a common limit capturing the exact behavior [Fig. 3(b)]. This makes evident the fact that knowledge of the behavior of correlations as $N\to\infty$ is not sufficient to conclude the correctness of mean-field theory or the convergence of higher-order cumulant expansions in this limit.

APPENDIX C: THIRD-ORDER CUMULANT EQUATIONS WITH SYMMETRY BREAKING

In this appendix we provide the results of third-order cumulant expansions with symmetry-breaking terms for the central spin and Tavis-Cummings models.

Retaining moments, e.g., $\langle\sigma_0^+\sigma_n^+\rangle$, in the equations of motion that would otherwise vanish under U(1) symmetry significantly increases the number of equations required to form a complete set at any given order. We used the QuantumCumulants.jl Julia package [35] to derive the third-order equations in each case. Using an initial state that breaks the symmetry, these equations were evolved to long times to obtain a numerical approximation of the steady state.

Since the coefficients of terms in the definition of a cumulant always sum to zero [cf. Eq. (A11)], when one sets a cumulant to zero to obtain an approximation for a high-order moment, the number of terms in the approximation for that moment, accounting for their signs, is 1. That is, provided no terms in the cumulant vanish due to symmetry considerations. As a result, in the presence of symmetry breaking there is no longer disparity between the asymptotic form of odd-order cumulant equations and mean-field theory as $N\to\infty$ due to the factorization of moments $\langle\sigma_0^+\sigma_n^-\sigma_m^+\sigma_k^-\ldots\rangle$.

In line with the above, Fig. 6(a) shows a common $N\to\infty$ limit for the third-order equations with symmetry breaking (dotted line) and mean-field theory. Note, however, there is a range of N [$N\leqslant 26$ in Fig. 6(a)] for which symmetry breaking is not present in the obtained steady state [Fig. 6(b)] and the original third-order results are followed by the dotted line. Further, even with symmetry breaking the third-order results cannot be relied upon to provide a better approximation than a second-order expansion. This is clearly seen in Fig. 6(c), which shows $p_0^\uparrow$ against $\Gamma_\uparrow/\Gamma_\downarrow$ at $N=50$. We point out the agreement of all cumulant expansions at pump strengths well below the mean-field threshold, where $p_0^\uparrow$ must vanish as $N\to\infty$. Note also the crossing of the third-order (symmetry-preserving) and mean-field curves which marks the transition to the symmetry-broken steady state; this is inevitable at large N, where the third-order result is below the mean-field prediction.

Finally, in Fig. 6(d) we observe similar behavior with the third-order equations with symmetry-breaking terms for the Tavis-Cummings model, although in this case the mean-field limit is approached from below.

[1] A. S. Lilly Thankamony, J. J. Wittmann, M. Kaushik, and B. Corzilius, Dynamic nuclear polarization for sensitivity enhancement in modern solid-state NMR, Prog. Nucl. Magn. Reson. Spectrosc. **102-103**, 120 (2017).

[2] P. Fernández-Acebal, O. Rosolio, J. Scheuer, C. Müller, S. Müller, S. Schmitt, L. McGuinness, I. Schwarz, Q. Chen, A. Retzker, B. Naydenov, F. Jelezko, and M. Plenio, Toward hyperpolarization of oil molecules via single nitrogen vacancy centers in diamond, Nano Lett. **18**, 1882 (2018).

[3] T. Villazon, P. W. Claeys, A. Polkovnikov, and A. Chandran, Shortcuts to dynamic polarization, Phys. Rev. B **103**, 075118 (2021).

[4] R. Rizzato, F. Bruckmaier, K. S. Liu, S. J. Glaser, and D. B. Bucher, Polarization Transfer from Optically Pumped Ensembles of N-*V* Centers to Multinuclear Spin Baths, Phys. Rev. Appl. **17**, 024067 (2022).

[5] R. Schirhagl, K. Chang, M. Loretz, and C. L. Degen, Nitrogen-vacancy centers in diamond: Nanoscale sensors for physics and biology, Annu. Rev. Phys. Chem. **65**, 83 (2014).

[6] Y. Wu, F. Jelezko, M. B. Plenio, and T. Weil, Diamond quantum devices in biology, Angew. Chem. Int. Ed. **55**, 6586 (2016).

[7] R. D. Allert, K. D. Briegel, and D. B. Bucher, Advances in nano- and microscale NMR spectroscopy using diamond quantum sensors, Chem. Commun. **58**, 8165 (2022).

[8] J. M. Taylor, C. M. Marcus, and M. D. Lukin, Long-Lived Memory for Mesoscopic Quantum Bits, Phys. Rev. Lett. **90**, 206803 (2003).

[9] D. P. DiVincenzo, Double quantum dot as a quantum bit, Science **309**, 2173 (2005).

[10] F. H. L. Koppens, C. Buizert, K. J. Tielrooij, I. T. Vink, K. C. Nowack, T. Meunier, L. P. Kouwenhoven, and L. M. K. Vandersypen, Driven coherent oscillations of a single electron spin in a quantum dot, Nature (London) **442**, 766 (2006).

[11] R. Hanson, L. P. Kouwenhoven, J. R. Petta, S. Tarucha, and L. M. K. Vandersypen, Spins in few-electron quantum dots, Rev. Mod. Phys. **79**, 1217 (2007).

[12] P. C. Maurer, G. Kucsko, C. Latta, L. Jiang, N. Y. Yao, S. D. Bennett, F. Pastawski, D. Hunger, N. Chisholm, M. Markham, D. J. Twitchen, J. I. Cirac, and M. D. Lukin, Room-temperature quantum bit memory exceeding one second, Science **336**, 1283 (2012).

[13] L. Childress and R. Hanson, Diamond NV centers for quantum computing and quantum networks, MRS Bull. **38**, 134 (2013).

[14] J. Cai, A. Retzker, F. Jelezko, and M. B. Plenio, A large-scale quantum simulator on a diamond surface at room temperature, Nat. Phys. **9**, 168 (2013).

[15] P. Kirton, M. M. Roses, J. Keeling, and E. G. Dalla Torre, Introduction to the Dicke model: From equilibrium to

nonequilibrium, and *vice versa*, Adv. Quantum Technol. **2**, 1800043 (2019).
[16] M. Sánchez-Barquilla, R. E. F. Silva, and J. Feist, Cumulant expansion for the treatment of light-matter interactions in arbitrary material structures, J. Chem. Phys. **152**, 034108 (2020).
[17] P. M. Chaikin and T. C. Lubensky, *Principles of Condensed Matter Physics*, 1st ed. (Cambridge University Press, Cambridge, UK, 1995).
[18] T. J. Osborne and F. Verstraete, General Monogamy Inequality for Bipartite Qubit Entanglement, Phys. Rev. Lett. **96**, 220503 (2006).
[19] N. Makri, The linear response approximation and its lowest order corrections: An influence functional approach, J. Phys. Chem. B **103**, 2823 (1999).
[20] P. R. Eastham and P. B. Littlewood, Bose condensation of cavity polaritons beyond the linear regime: The thermal equilibrium of a model microcavity, Phys. Rev. B **64**, 235101 (2001).
[21] T. Mori, Exactness of the mean-field dynamics in optical cavity systems, J. Stat. Mech. (2013) P06005.
[22] F. Carollo and I. Lesanovsky, Exactness of Mean-Field Equations for Open Dicke Models with an Application to Pattern Retrieval Dynamics, Phys. Rev. Lett. **126**, 230601 (2021).
[23] E. Fiorelli, M. Müller, I. Lesanovsky, and F. Carollo, Mean-field dynamics of open quantum systems with collective operator-valued rates: Validity and application, New J. Phys. **25**, 083010 (2023).
[24] R. Kubo, Generalized cumulant expansion method, J. Phys. Soc. Jpn. **17**, 1100 (1962).
[25] J. Fricke, Transport equations including many-particle correlations for an arbitrary quantum system: A general formalism, Ann. Phys. **252**, 479 (1996).
[26] A. Vardi and J. R. Anglin, Bose-Einstein Condensates beyond Mean Field Theory: Quantum Backreaction as Decoherence, Phys. Rev. Lett. **86**, 568 (2001).
[27] T. Köhler and K. Burnett, Microscopic quantum dynamics approach to the dilute condensed Bose gas, Phys. Rev. A **65**, 033601 (2002).
[28] M. Kira and S. W. Koch, Cluster-expansion representation in quantum optics, Phys. Rev. A **78**, 022102 (2008).
[29] S. Krämer and H. Ritsch, Generalized mean-field approach to simulate the dynamics of large open spin ensembles with long range interactions, Eur. Phys. J. D **69**, 282 (2015).
[30] P. Kirton and J. Keeling, Superradiant and lasing states in driven-dissipative Dicke models, New J. Phys. **20**, 015009 (2018).
[31] F. Reiter, T. L. Nguyen, J. P. Home, and S. F. Yelin, Cooperative Breakdown of the Oscillator Blockade in the Dicke Model, Phys. Rev. Lett. **125**, 233602 (2020).
[32] K. B. Arnardottir, A. J. Moilanen, A. Strashko, P. Törmä, and J. Keeling, Multimode Organic Polariton Lasing, Phys. Rev. Lett. **125**, 233603 (2020).
[33] F. Robicheaux and D. A. Suresh, Beyond lowest order mean-field theory for light interacting with atom arrays, Phys. Rev. A **104**, 023702 (2021).
[34] H. Wang and M. Blencowe, Coherently amplifying photon production from vacuum with a dense cloud of accelerating photodetectors, Commun. Phys. **4**, 128 (2022).
[35] D. Plankensteiner, C. Hotter, and H. Ritsch, QuantumCumulants.jl: A Julia framework for generalized mean-field equations in open quantum systems, Quantum **6**, 617 (2022).
[36] K. J. Kusmierek, S. Mahmoodian, M. Cordier, J. Hinney, A. Rauschenbeutel, M. Schemmer, P. Schneeweiss, J. Volz, and K. Hammerer, Higher-order mean-field theory of chiral waveguide QED, SciPost Phys. Core **6**, 041 (2023).
[37] N. Werren, E. M. Gauger, and P. Kirton, A quantum model of lasing without inversion, New J. Phys. **24**, 093027 (2022).
[38] Y.-X. Huang, M. Li, K. Lin, Y.-L. Zhang, G.-C. Guo, and C.-L. Zou, Classical-to-quantum transition in multimode nonlinear systems with strong photon-photon coupling, Phys. Rev. A **105**, 043707 (2022).
[39] O. Rubies-Bigorda, S. Ostermann, and S. F. Yelin, Characterizing superradiant dynamics in atomic arrays via a cumulant expansion approach, Phys. Rev. Res. **5**, 013091 (2023).
[40] M. W. Doherty, N. B. Manson, P. Delaney, F. Jelezko, J. Wrachtrup, and L. C. Hollenberg, The nitrogen-vacancy colour centre in diamond, Phys. Rep. **528**, 1 (2013).
[41] G. Chen, D. L. Bergman, and L. Balents, Semiclassical dynamics and long-time asymptotics of the central-spin problem in a quantum dot, Phys. Rev. B **76**, 045312 (2007).
[42] L. P. Lindoy and D. E. Manolopoulos, Simple and Accurate Method for Central Spin Problems, Phys. Rev. Lett. **120**, 220604 (2018).
[43] P. Ribeiro and T. Prosen, Integrable Quantum Dynamics of Open Collective Spin Models, Phys. Rev. Lett. **122**, 010401 (2019).
[44] A. Ricottone, Y. N. Fang, and W. A. Coish, Balancing coherent and dissipative dynamics in a central-spin system, Phys. Rev. B **102**, 085413 (2020).
[45] T. Villazon, A. Chandran, and P. W. Claeys, Integrability and dark states in an anisotropic central spin model, Phys. Rev. Res. **2**, 032052(R) (2020).
[46] D. Malz, R. Trivedi, and J. I. Cirac, Large-N limit of Dicke superradiance, Phys. Rev. A **106**, 013716 (2022).
[47] B. A. Chase and J. M. Geremia, Collective processes of an ensemble of spin-1/2 particles, Phys. Rev. A **78**, 052101 (2008).
[48] M. Xu, D. A. Tieri, and M. J. Holland, Simulating open quantum systems by applying SU(4) to quantum master equations, Phys. Rev. A **87**, 062101 (2013).
[49] F. Damanet, D. Braun, and J. Martin, Master equation for collective spontaneous emission with quantized atomic motion, Phys. Rev. A **93**, 022124 (2016).
[50] M. Gegg and M. Richter, Efficient and exact numerical approach for many multi-level systems in open system CQED, New J. Phys. **18**, 043037 (2016).
[51] P. Kirton and J. Keeling, Suppressing and Restoring the Dicke Superradiance Transition by Dephasing and Decay, Phys. Rev. Lett. **118**, 123602 (2017).
[52] N. Shammah, S. Ahmed, N. Lambert, S. De Liberato, and F. Nori, Open quantum systems with local and collective incoherent processes: Efficient numerical simulations using permutational invariance, Phys. Rev. A **98**, 063815 (2018).
[53] C. Gardiner, *Stochastic Methods: A Handbook for the Natural and Social Sciences*, 4th ed., Springer Series in Synergetics Vol. 13 (Springer, New York, 2009).
[54] C. Weedbrook, S. Pirandola, R. García-Patrón, N. J. Cerf, T. C. Ralph, J. H. Shapiro, and S. Lloyd, Gaussian quantum information, Rev. Mod. Phys. **84**, 621 (2012).
[55] R. Frantzeskakis, J. Van Dyke, L. Zaporski, D. A. Gangloff, C. L. Gall, M. Atatüre, S. E. Economou, and E. Barnes,

Time-crystalline behavior in central-spin models with Heisenberg interactions, Phys. Rev. B **108**, 075302 (2023).

[56] M. Krishna, P. Solanki, M. Hajdušek, and S. Vinjanampathy, Measurement-Induced Continuous Time Crystals, Phys. Rev. Lett. **130**, 150401 (2023).

[57] We have checked this explicitly up to 14th order.

[58] As mentioned in the paper, working with the cumulant equations by counting operators a requires treating multiple photon operators as distinct objects when breaking higher-order moments to obtain a closed set of equations. Alternatively, one can consider a truncation of the photon space to $N_{\text{phot.}}$ levels and work, e.g., in the basis of generalized Gell-Mann matrices. This increases the number of equations at any order of expansion but removes the reliance on additional assumptions, i.e., Gaussianity.

[59] M. Tavis and F. W. Cummings, Exact Solution for an N-Molecule-Radiation-Field Hamiltonian, Phys. Rev. **170**, 379 (1968).

[60] D. D. B. Rao, A. Ghosh, D. Gelbwaser-Klimovsky, N. Bar-Gill, and G. Kurizki, Spin-bath polarization via disentanglement, New J. Phys. **22**, 083035 (2020).

[61] C. W. Lai, P. Maletinsky, A. Badolato, and A. Imamoglu, Knight-Field-Enabled Nuclear Spin Polarization in Single Quantum Dots, Phys. Rev. Lett. **96**, 167403 (2006).

[62] K. A. Al-Hassanieh, V. V. Dobrovitski, E. Dagotto, and B. N. Harmon, Numerical Modeling of the Central Spin Problem Using the Spin-Coherent-State *P* Representation, Phys. Rev. Lett. **97**, 037204 (2006).

[63] B. Fauseweh, P. Schering, J. Hüdepohl, and G. S. Uhrig, Efficient algorithms for the dynamics of large and infinite classical central spin models, Phys. Rev. B **96**, 054415 (2017).

[64] R. Röhrig, P. Schering, L. B. Gravert, B. Fauseweh, and G. S. Uhrig, Quantum mechanical treatment of large spin baths, Phys. Rev. B **97**, 165431 (2018).

[65] X. Zhou, Q.-K. Wan, and X.-H. Wang, Many-body dynamics and decoherence of the XXZ central spin model in external magnetic field, Entropy **22**, 23 (2019).

[66] E. M. Kessler, G. Giedke, A. Imamoglu, S. F. Yelin, M. D. Lukin, and J. I. Cirac, Dissipative phase transition in a central spin system, Phys. Rev. A **86**, 012116 (2012).

[67] J. Hildmann, E. Kavousanaki, G. Burkard, and H. Ribeiro, Quantum limit for nuclear spin polarization in semiconductor quantum dots, Phys. Rev. B **89**, 205302 (2014).

[68] M. Bortz and J. Stolze, Spin and entanglement dynamics in the central-spin model with homogeneous couplings, J. Stat. Mech. (2007) P06018.

[69] D. Stanek, C. Raas, and G. S. Uhrig, Exact dynamics of XX central spin models, Phys. Scr. **2009**, 014049 (2009).

[70] D. Stanek, C. Raas, and G. S. Uhrig, From quantum-mechanical to classical dynamics in the central-spin model, Phys. Rev. B **90**, 064301 (2014).

[71] S. Bhattacharya and S. Banerjee, Revisiting the quantum open system dynamics of central spin model, Quanta **10**, 55 (2021).

[72] L.-H. Tang, D. M. Long, A. Polkovnikov, A. Chandran, and P. W. Claeys, Integrability and quench dynamics in the spin-1 central spin XX model, SciPost Phys. **15**, 030 (2023).

[73] F. Carollo, Non-Gaussian dynamics of quantum fluctuations and mean-field limit in open quantum central spin systems, arXiv:2305.15547.

[74] S. Mahmoodian, G. Calajó, D. E. Chang, K. Hammerer, and A. S. Sørensen, Dynamics of Many-Body Photon Bound States in Chiral Waveguide QED, Phys. Rev. X **10**, 031011 (2020).

[75] P. Fowler-Wright, J. Keeling, P. Kirton, B. W. Lovett, and K. B. Arnardottir, Data underpinning determining the validity of cumulant expansions for central spin models (2023), doi:10.17630/e1f1b609-f324-4b7c-9b7a-9cd4655b8b5d.